Effect of softness of the potential on the stress anisotropy in liquids

José Alejandre, Fernando Bresme, Minerva González-Melchor, and Fernando del Río

Citation: The Journal of Chemical Physics **126**, 224511 (2007); doi: 10.1063/1.2738475
View online: http://dx.doi.org/10.1063/1.2738475
View Table of Contents: http://scitation.aip.org/content/aip/journal/jcp/126/22?ver=pdfcov
Published by the AIP Publishing

Effect of softness of the potential on the stress anisotropy in liquids

José Alejandre
Departamento de Química, Universidad Autónoma Metropolitana-Iztapalapa, Avenida San Rafael Atlixco 186, Col. Vicentina, 09340 Mexico D.F., México and Department of Chemistry, University of Cambridge, Lensfield Road, Cambridge CB2 1EW, United Kingdom

Fernando Bresme
Department of Chemistry, Imperial College London, Exhibition Road, London SW7 2AZ, United Kingdom

Minerva González-Melchor
Instituto de Física, Universidad Autónoma de Puebla, Apartado Postal J-48, 72570 Puebla, Mexico

Fernando del Río
Departamento de Física, Universidad Autónoma Metropolitana-Iztapalapa, Avenida San Rafael Atlixco 186, Col. Vicentina, 09340 Mexico D.F., México

(Received 17 January 2007; accepted 18 April 2007; published online 12 June 2007)

We have performed molecular dynamics simulations of dense liquids using nonconformal and Gaussian potential models. We investigate the effect of the softness of the potential on the pressure tensor of liquids and dense fluids when the simulations are carried out using parallelepiped cells. The combination of periodic boundary conditions and small cross sectional areas induces an anisotropy in the diagonal components of the pressure tensor. This anisotropy results in an artificial stress in the system that has to be taken into account in simulations of explicit interfaces, where the artificial stress introduces errors in the computation of the surface tension. At high liquid densities the stress anisotropy exhibits an oscillatory dependence with the cross sectional area of the simulation box. We find that the softness of the potential has a dramatic effect on the amplitude of the oscillations, which can be significantly reduced in soft potentials, such as those used in the modeling of hydrocarbon liquids or polymers. © *2007 American Institute of Physics*.
[DOI: 10.1063/1.2738475]

I. INTRODUCTION

The influence of finite size effects in the computer simulation of dense fluids has been investigated in several works over the last four decades.[1–4] Kolafa *et al.*[5,6] investigated the *periodic error*, which is characterized by an oscillatory dependence of the pressure with system size. The oscillations in the pressure are connected to the structure of the fluid. We have recently found in simulations performed with noncubic boxes of parallelepiped shape that the diagonal components of the pressure tensor are not isotropic.[7] The degree of anisotropy is strongly dependent on the cross sectional area of the simulation box, and it is particularly significant for box lengths smaller than ten times the particle diameter. The anisotropy of the components of the pressure tensor results then in an artificial stress[7] in the system. The stress oscillates with the cross sectional area and the amplitude of the oscillations decays to zero for large areas. Simulations of explicit interfaces, liquid-vapor and liquid-liquid, are normally performed in parallelepiped simulation boxes. Therefore the computation of the surface tension in such geometries using small system sizes is prone to include errors associated to the lack of isotropy of the pressure tensor.

González-Melchor *et al.*[8] have reported an oscillatory surface tension with surface area for ionic liquid interfaces and Orea *et al.*[9] have found a similar trend for Lennard-Jones (LJ) and square well potentials. The potential models used in the simulation of ionic liquids feature a strong repulsion interaction, $\propto 1/r^{225}$ at short interparticle distances r. Likewise, Lennard-Jones potentials also exhibit a relatively strong repulsion, $1/r^{12}$ at short interparticle distances. On the other hand, the repulsive forces normally used in dissipative particle dynamics[10,11] (DPD) decay linearly with r. Using DPD Velázquez *et al.*[12] have reported, very recently, the absence of stress anisotropy in bulk liquid phases and in liquid-liquid interfaces. In the latter case the interfacial tension was essentially independent on the surface area. It is important to note that the interactions in these systems were modeled with purely repulsive soft forces, which do not lead to significant structure, and consequently the stress anisotropy effect is suppressed. The connection between the stress anisotropy resulting from finite size effects and the softness of the potential has not been established. Such study is necessary to address the importance of finite size effects in the simulations of complex interfaces, such as those involving polymeric species.

Velázquez *et al.*[12] also performed DPD simulations of dense phases using soft attractive potentials by including three body effects.[13,14] Unlike the repulsive DPD fluid, the introduction of attractive interactions enhances the fluid structure, which is characterized by an oscillatory radial distribution function. It was found that in this case the pressure tensor components show the same anisotropy as discussed in ionic and LJ potentials. This suggest that the fluid structure plays an important role in inducing the pressure tensor an-

isotropy. Therefore, one question of interest in the simulation of dense liquids is to what extent the pressure tensor anisotropy is modified by the softness of the repulsive contribution to the potential. We address this question in this paper.

The stress anysotropy influences the calculation of the interfacial surface tensions. The surface tension is important in many applications, it is then convenient to understand the conditions where the finite size effects inducing the pressure tensor anisotropy can be neglected in order to avoid any artificial stress anisotropy in the system. One would expect that the finite size effects on stress anisotropy as a function of transversal area become less relevant as the system becomes structureless. To prove this idea we investigate here two types of soft potentials: a Gaussian attractive model and the so called approximate nonconformal (ANC) potential.[15] Two different potentials $u_1(r;\epsilon_1,\sigma_1)$ and $u_2(r;\epsilon_2,\sigma_2)$, where ϵ_i and σ_i are, respectively, the characteristic energy and length, are said to be conformal whenever their reduced forms $u_i^*=u_i(r/\sigma_i)/\epsilon_i$ are equal to each other, that is, when $u_1^*(r^*)=u_2^*(r^*)$. Conformality between the potentials of two fluids implies that they follow the principle of corresponding states, so that their reduced thermodynamic properties, at equal reduced states, are themselves equal. The potentials of real substances, e.g., atomic and polymeric, are not conformal in general. The ANC potential takes into account the nonconformality of interactions of real molecules in the gaseous phase in a systematic way by means of one parameter, called the softness s. The three-parameter (s,ϵ,σ) ANC potentials have been used to calculate the second virial coefficient and zero-pressure viscosity coefficients of single components and mixtures in the gaseous phase.[15–17] These properties agree with experimental data within their estimated error. The ANC potential has also been used to study the dependence of the phase equilibria and interfacial properties[18] with the potential softness finding that the critical temperature increases with softness. The ANC potential functions can be used as reliable effective interactions for real dense fluids. Typical values for real molecules[16] are $s=0.5$ for *n*-hexane, $s=0.7$ for *n*-propane, and $s=0.9$ for methane. Details about the ANC potential can be found in Ref. 15.

The paper is organized as follows: Section II describes the potential model and discusses the computation of the different properties investigated in the paper. Section III provides some details of the simulation and the discussion of our results. Finally, the conclusions and further comments close the paper.

II. POTENTIAL MODELS AND CALCULATED PROPERTIES

The ANC interaction potential[15] $u_{\mathrm{ANC}}(r,s)$ is defined in reduced form $u^*=u/\epsilon$ as a modified Kihara function

$$u^*(r^*;s)=\left(\frac{1-a}{\zeta(r^*,s)-a}\right)^{12}-2\left(\frac{1-a}{\zeta(r^*,s)-a}\right)^{6}, \tag{1}$$

with $a=0.095\,74$ and

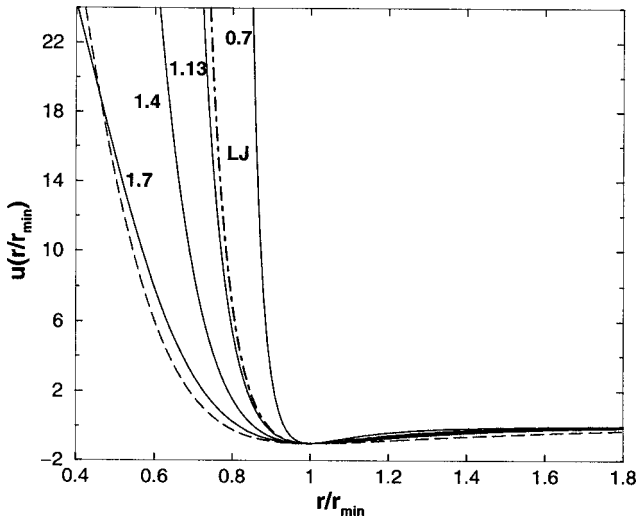

FIG. 1. Plot of potential functions with various degrees of softness. The solid curves stand for ANC potentials with $s=0.7$, 1.13, 1.4, and 1.7 as labeled. The Gaussian potential is shown by the dashed curve that runs close to the $s=1.7$ curve. The Lennard-Jones potential is shown by the dot-dashed line.

$$\zeta^3(r^*,s)=r^{*3}/s+1-1/s, \tag{2}$$

where $r^*=r/r_{\mathrm{min}}$ (r is the distance between two particles and r_{min} is the position where the potential is minimum), ϵ is the depth of the potential well, and s is the softness parameter. The spherical Kihara and hard-sphere potentials are obtained from $u(r^*;s)$ for $s=1$ and $s\to 0$, respectively. The value of a was chosen to make the reference potential $u_0(r^*)=u(r^*;s=1)$ closely conformal to the argon-argon pair interaction. The Lennard-Jones 12/6 potential function (LJ-12/6) has a softness $s=1.13$. The distance $r_{\mathrm{min}}=2^{1/6}\sigma_{\mathrm{LJ}}$, where σ_{LJ} is the distance where the LJ potential is zero.

The Gaussian model contains a repulsive and attractive contributions modeled through two exponentials and it is defined as

$$u_G(r)=Ae^{-(ar)^2}-Be^{-(br)^2}, \tag{3}$$

where $a=2.02/\sigma_G$, $b=0.63/\sigma_G$, $A=85.2\epsilon$, and $B=2.13\epsilon$ are constants. Here σ_G is the distance at which the potential is zero and $-\epsilon$ is the interaction strength. Actually this Gaussian potential can be approximated by an ANC function with softness $s=1.7$. Both potentials are finite at $r=0$ and are shown in Fig. 1.

The main quantity we will discuss in this work is the *stress anisotropy*, denoted by γ. Even though the system is homogeneous we have followed the definition employed in the computation of the surface tension of planar liquid-vapor interfaces in terms of the components of the pressure tensor. Thus the stress anisotropy of our systems is given by

$$\gamma=L_z\{\langle P_{zz}\rangle-0.5[\langle P_{xx}\rangle+\langle P_{yy}\rangle]\}, \tag{4}$$

where L_z is the box length of the simulation cell in the z direction. This quantity measures the deviations from the isotropy in the system, which emerges when a noncubic cell is used in the simulation or when interactions in the system are not soft enough to supress the structure of the system. The diagonal components of the pressure tensor P_{xx}, P_{yy}, and

P_{zz} are obtained using the mechanical definition,

$$P_{zz} = \rho k_B T + \frac{1}{V} \sum_{i}^{N-1} \sum_{j>i}^{N} z_{ij} F_{ij}^{z}, \tag{5}$$

where P_{zz} is the zz component of the pressure tensor. $z_{ij}=z_i - z_j$, z_i being the z coordinate of atom i, $\rho=N/V$ is the particle number density, T is the absolute temperature, and k_B is the Boltzmann's constant. The force component between atoms i and j in the z direction is

$$F_{ij}^{z} = -\frac{du(r)}{dr}\frac{z_{ij}}{r}, \tag{6}$$

where $u(r)$ can be either $u^*(r^*;s)$ or $u_G(r)$.

In a homogeneous fluid the three components of the pressure tensor must have the same value, and γ has to be zero, within statistical error. We have shown[7] that this is not true when simulations are performed using small noncubic cells. In this case the stress anisotropy oscillates with the cross sectional area of the simulation cell.

In order to compare the stress anisotropies of the different potentials, which have different critical temperatures we use a corresponding state expression[19] for the reduced stress anisotropy,

$$\gamma_R = \frac{\gamma}{\rho_c^{2/3} k_B T_c}, \tag{7}$$

where ρ_c and T_c are the critical density and temperature, respectively. The stress anisotropy for the Gaussian potential is represented in standard reduced units, $\gamma^* = \gamma\sigma_G^2/\epsilon$.

III. RESULTS

Molecular dynamics simulations at constant number of particles N, volume V, and temperature T were performed. Three types of simulations were carried out for the ANC potential: (a) interface simulations using $s=1.4$ to calculate the phase diagram at the liquid-vapor equilibrium, (b) liquids in cubic boxes to obtain the radial distribution function, and (c) liquids in parallelepiped cells to calculate the stress anisotropy. For the Gaussian model we only performed simulations on a dense fluid phase using cubic and noncubic boxes.

The liquid-vapor phase diagram of fluids interacting through the ANC potential has been reported by del Río *et al.*[18] for softness going from 0.5 to 1.0. In order to locate the phase boundaries of a softer potential, $s=1.4$, we performed simulations of the liquid-vapor interface as a function of the temperature following the same procedure as del Río *et al.* The simulation consisted of $N=2000$ particles in a simulation cell with dimensions $L_x^*=L_x/r_{\min}=L_y^*=9.8$, $L_z^*=53.45$, and the forces were truncated at $r_c=2.227r_{\min}$. The reduced density and temperature are $\rho_{\mathrm{ANC}}^*=\rho r_{\min}^3$ and $T^*=k_BT/\epsilon$, respectively. Figure 2 shows the phase diagram for the ANC potential with softness $s=0.7$ and $s=1.4$. As shown previously,[18] the critical temperature increases by increasing s.

The radial distribution function for the ANC potential in terms of s is shown in Fig. 3(a) for systems at $T/T_c=1.54$ and $\rho/\rho_c=2.29$. Both states are in the one phase region and the results show a liquidlike structure. As expected, the fluid with $s=1.4$ is less structured and the particles overlap more at short distances than those with $s=0.7$. Figure 3(b) shows the results for the Gaussian model at $T^*=1.32$ and $\rho^*=1.61$. At this density the fluid exhibits a rather marked structure, resembling the pair correlation function of a dense fluid. Nonetheless, the fact that the Gaussian model corresponds approximately to an ANC potential with $s=1.7$ would lead us to expect that, at equivalent densities, the Gaussian model

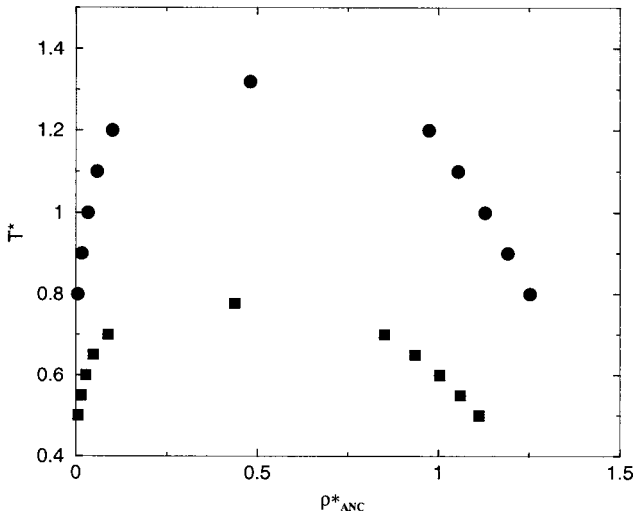

FIG. 2. Orthobaric curves T^* against ρ_{ANC}^* of ANC fluids. Filled circles are results from this work for $s=1.4$ and filled squares are results taken from del Río *et al.* work (Ref. 18) for $s=0.7$.

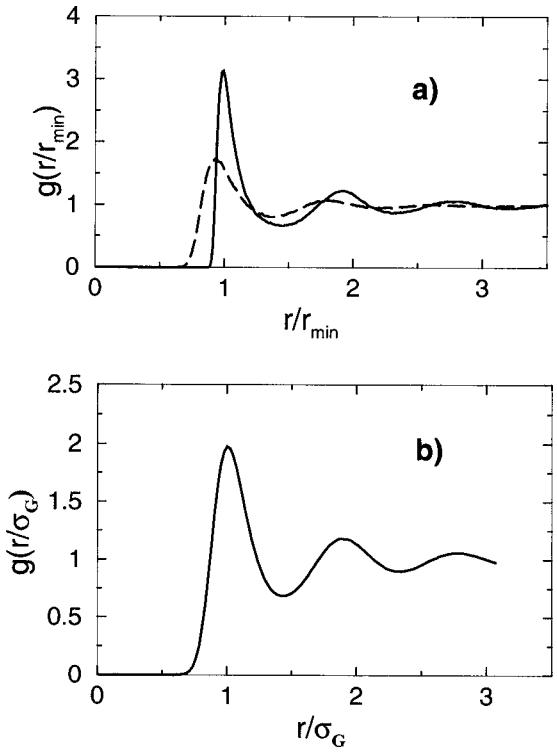

FIG. 3. Radial distribution functions: (a) ANC potential at $T/T_c=1.54$ and $\rho/\rho_c=2.29$. The continuous line is for $s=0.7$ and the dashed line for $s=1.4$. (b) Gaussian potential at $T_G^*=1.32$ and $\rho_G^*=1.61$. The simulations were performed using 500 molecules.

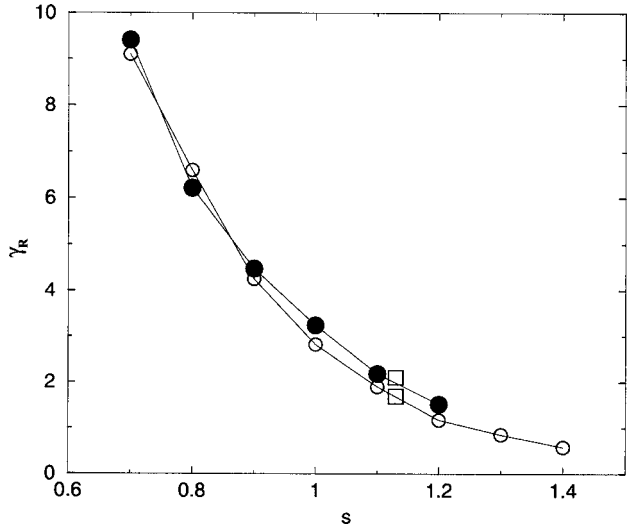

FIG. 4. Stress anisotropy as a function of softness. $L_x=4.5702r_{\min}$ and $\rho^*_{\mathrm{ANC}}=1.1314$. The ANC results are shown at $T^*=0.8$ (filled circles) and $T^*=1.2$ (open circles), and LJ model (open squares) for both temperatures.

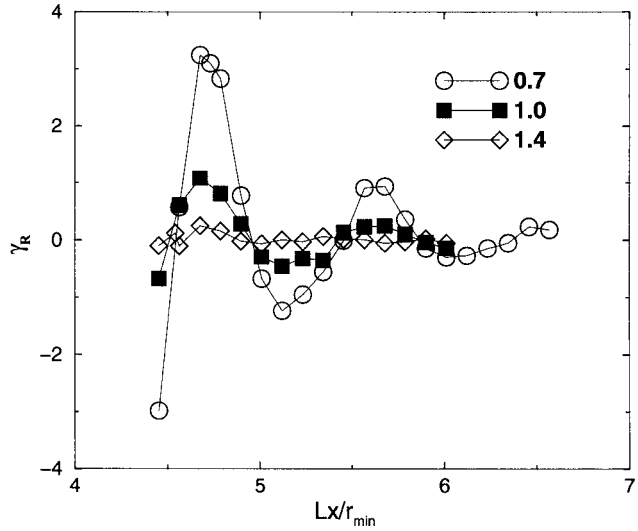

FIG. 5. Reduced stress anisotropy as a function of L^*_x for the ANC potential at $T^*=1.2$ and $\rho^*_{\mathrm{ANC}}=1.0$. The softness is shown in the figure.

should have a structure closer to that of the softer ANC system shown in Fig. 3(a). And indeed, comparing the maximum values $g_{\max}$ of $g(r)$ in Figs. 3(a) and 3(b) it is seen that the Gaussian case, $g_{\max}\simeq 2$, is perhaps closer to the ANC potential with $s=1.4$, with $g_{\max}\simeq 1.7$, than to the harder ANC fluid that has $g_{\max}\simeq 3$.

In a previous work González-Melchor *et al.*[7] investigated the stress anisotropy of the spherically truncated and shifted (cutoff$=2.5\sigma_{\mathrm{LJ}}$) Lennard-Jones potential. The simulations were performed at densities typical of a liquid $\rho^*_{\mathrm{LJ}}=\rho\sigma^3_{\mathrm{LJ}}=0.8$. In this case γ oscillated around zero with the cross sectional area of the simulation box. The oscillations attained a maximum at $L_x=5.13\sigma_{\mathrm{LJ}}=4.5703r_{\min}$ and its amplitude decreased by 20% in the interval of temperatures $T/T_c=0.7-1$.

To analyze the effect of the softness on the stress anisotropy and to compare with the results for the LJ potential ($s=1.13$), we performed simulations in parallelepiped cells at constant volume using the ANC model with $N=500$ at the same conditions as those used for the LJ potential, i.e., $L_x=4.5703r_{\min}$ and $\rho^*_{\mathrm{ANC}}=1.1314$. The value of $L_z=18.2810r_{\min}$ was used in all simulations. The results were obtained at $T^*=0.8$ and $T^*=1.2$, same values as those used in the LJ calculations. These termodynamic states are in the one phase region. To avoid the two phase region, s was set to 1.2 at the lowest temperature. The critical temperature of $s=0.8$, 1.2, and 1.3 were estimated from a quadratic regression $T^*_c=0.066+1.166s+0.176s^2$ obtained from published results[18] and the calculated value at $s=1.4$ in this work. The results of γ_R as a function of softness are shown in Fig. 4. Clearly γ_R decreases when s is increased. The value of γ_R at $s=0.7$ is around six times greater than its value at $s=1.2$ for systems with $T^*=0.8$ ($T/T_c=1.03$). The stress anisotropy also decreases with temperature for $s>0.9$. For instance at $s=1.2$ and $T^*=0.8$ ($T/T_c=0.7$), γ_R is 1.3 times larger than the anisotropy at $T^*=1.2$ ($T/T_c=0.99$). The change in temperature is small as compared with the change due to the softness of the potential, see Fig. 4. A softer potential leads to a smaller artificial effect on stress anisotropy.

Simulations of ANC potential on parallelepiped cells at different cross sectional areas were performed using 500 particles and $\rho^*_{\mathrm{ANC}}=1.0$ at $T^*=1.2$ for $s=0.7$, 1.0, and 1.4. This state is in the one phase region for all the softness values as can be seen in Fig. 2. The dimension of the longest length of the simulation cell was $L^*_x=N/(\rho^*_{\mathrm{ANC}}A^*)$. Figure 5 shows γ_R as a function of $L_x/r_{\min}$ for models having larger and smaller softness than the LJ potential ($s=1.13$). The wavelength is around $r_{\min}$ and the maxima are around the same value because all the ANC potentials have the minima at the same distance. The amplitude of the stress anisotropy is greater in harder potentials. The oscillations are damped faster in softer models and approach zero at large box length distances.

For the Gaussian model we have considered simulation boxes containing 2744 particles. The reduced density $\rho^*_G=\rho\sigma^3_G$ and temperature $T^*=k_BT/\epsilon$ were 1.61 and 1.32, respectively. These conditions result in a structure that resembles a dense liquid. Despite the fact that the repulsive part is very soft as it is modeled by a Gaussian function, we

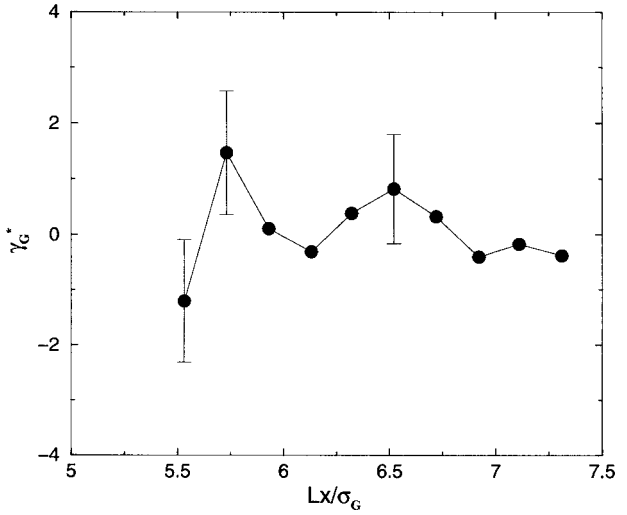

FIG. 6. Stress anisotropy for the Gaussian model as a function of L^*_x for the Gaussian model at $T^*=1.32$ and $\rho^*_G=1.61$.

do still observe anisotropy in the pressure tensor diagonal elements, which results again in oscillations in the stress anisotropy. A plot of γ_G^* as a function of L_x/σ_G is shown in Fig. 6. This result emphasizes the relevance of the liquid structure in determining the stress anisotropy. We expect that such anisotropy will be observed in simulations of polymeric structures, which consider models based on Gaussian potentials.

IV. CONCLUSIONS

By using the ANC and Gaussian potentials, we have found that the softness of the potential plays an important role in determining the magnitude of the stress anisotropy observed in the computer simulations performed in noncubic boxes. The simulation results show that by increasing the softness, the anisotropy oscillates around zero with lower amplitude and the oscillations decay faster. These findings also show that finite size effects on transversal area are related with the structure of the fluid. When the fluid becomes structureless the finite size effects on the components of the pressure tensor are not relevant and small systems can be used to calculate interfacial properties without adding any spurious effect on the surface tension. The ANC potential might be a useful tool to quantify the softness of fluids at high density and explore the conditions needed to avoid finite size effects in the computation of interfacial properties.

ACKNOWLEDGMENTS

Two of the authors (J.A. and F.B.) would like to thank The Royal Society London and the Academia Mexicana de Ciencias for financial support. One of the authors (J.A.) wishes to thank Imperial College-London for the facilities provided during his stay at the Chemistry Department. He also acknowledges Professor J.-P. Hansen for his hospitality at Cambridge University and for financial support through the Schlumberger Visiting Fellow program. Another author (M.G.M.) is grateful to UAM-Iztapalapa for the support given as a visiting researcher in the Physics Department. Another author (F.D.R.) thanks Conacyt for financial support.

[1] J. L. Lebowitz and J. K. Percus, Phys. Rev. **124**, 1673 (1961).
[2] M. J. Mandell, J. Stat. Phys. **15**, 299 (1976).
[3] L. W. Pratt and S. W. Haan, J. Chem. Phys. **74**, 1873 (1981).
[4] L. W. Pratt and S. W. Haan, J. Chem. Phys. **74**, 1864 (1981).
[5] J. Kolafa, Mol. Phys. **75**, 577 (1992).
[6] J. Kolafa, S. Lavík, and A. Malijevský, Phys. Chem. Chem. Phys. **6**, 2335 (2004).
[7] M. González-Melchor, P. Orea, J. López-Lemus, F. Bresme, and J. Alejandre, J. Chem. Phys. **122**, 094503 (2005).
[8] M. González-Melchor, F. Bresme, and J. Alejandre, J. Chem. Phys. **122**, 104710 (2005).
[9] P. Orea, J. López-Lemus, and J. Alejandre, J. Chem. Phys. **123**, 114702 (2005).
[10] P. J. Hoogerbrugge and J. M. V. A. Koelman, Europhys. Lett. **19**, 155 (1992).
[11] R. D. Groot and P. B. Warren, J. Chem. Phys. **107**, 4423 (1997).
[12] M. E. Velázquez, A. Gama, M. González-Melchor, M. Neria, and J. Alejandre, J. Chem. Phys. **124**, 84104 (2005).
[13] I. Pagonabarraga and D. Frenkel, J. Chem. Phys. **115**, 5015 (2001).
[14] S. Y. Trofimov, E. L. F. Nies, and M. A. J. Michels, J. Chem. Phys. **117**, 9383 (2002).
[15] F. del Río, J. E. Ramos, and I. A. McLure, J. Phys. Chem. B **102**, 10568 (1998).
[16] J. E. Ramos, F. del Río, and I. A. McLure, J. Phys. Chem. B **102**, 10576 (1998).
[17] F. del Río, B. Ibarra, and L. Mier y Terán, Mol. Phys. **101**, 2997 (2003).
[18] F. del Río, E. Díaz-Herrera, E. Ávalos, and J. Alejandre, J. Chem. Phys. **122**, 034504 (2005).
[19] E. A. Guggenheim, J. Chem. Phys. **13**, 253 (1945).